JOURNAL OF SOLID STATE CHEMISTRY 69, 343–354 (1987)

Electron Irradiation Effects in (Cs,Ba)-Hollandites

L. A. BURSILL

School of Physics, University of Melbourne, Parkville, 3052, Victoria, Australia

AND DAVID J. SMITH

Centre for Solid State Science and Department of Physics, Arizona State University, Tempe, Arizona 85287

Received July 14, 1986; in revised form December 23, 1986

High-resolution electron microscopy examination of mixed (Cs,Ba)-hollandites reveals evidence for significant short-range order in the distribution of cation vacancies in the incompletely occupied tunnels. The structure was observed to be quite unstable under 400-keV electron irradiation after only a few minutes' study at a dose rate of ca. 10^4 electrons $Å^{-2}$ sec^{-1}. Transformations to a microtwinned phase having interaxial angles of 80°/110° rather than 90°, and finally to an amorphous substance, were directly observed and recorded using video techniques. It is evident that hollandites are structurally, chemically, and mechanically unstable under intense electron irradiation. The significance of these observations to the possible effects of self-irradiation in SYNROC preparations, where radioactive $^{137}Cs^{+1}$ transmites to $^{137}Ba^{2+}$ by electron decay, is discussed. © 1987 Academic Press, Inc.

Introduction

The preferred compositions for synthetic hollandite-type phases, designed for immobilization of radioactive ^{137}Cs, include the hollandite $(Cs_x,Ba_y)Al_{x+2y}Ti_{8-x-y}O_{16}$, with $x + y = 1.20$ and $x/y = 0.30$ (*1*), and the priderite $Cs_xAl_xTi_{8-x}O_{16}$, $1.5 \leq x \leq 2$ (*2*). Experimental studies of the possible effects of transmutation-induced structural transformations, due to the radioactive chemical change $^{137}Cs \rightarrow {}^{137}Ba + \beta^-$ (half-life $\tau_{1/2} =$ 30 years), have been sadly lacking in the literature. As pointed out in Ref. (*3*), replacement of monovalent Cs^{1+} by divalent Ba^{2+} must be accompanied by, for example, reduction of $Ti^{4+} + \beta^- \rightarrow Ti^{3+}$, which may lead to structural and mechanical instability and increased Cs^{1+} leachability of the hollandite or priderite phases. In addition, the direct effects of electron irradiation, due to the 0.518- and 1.218-MeV electrons emitted inside the solid, need to be investigated from the point of view of chemical, structural, and mechanical stability of the radioactive host. The long-term effects of such self-irradiation have either not been studied experimentally or else not yet reported in the literature. It has been assumed, so far, that Cs^{1+} substitutes randomly for Ba^{2+} in the hollandite phase (*4, 5*). Neither the long-term thermal stability nor electron irradiation "hardness" of mixed (Cs,Ba)-hollandites has been studied systematically (*3*).

In this paper, we report a high-resolution

0022-4596/87 $3.00
Copyright © 1987 by Academic Press, Inc.
All rights of reproduction in any form reserved.

electron microscopic (HREM) study of the mixed (Cs,Ba)-hollandite phase, when it was intended to search for evidence of short-range order, or possibly phase separation, in the (Cs,Ba) distribution. At the same time, we have unavoidably been led to study the effects of a relatively high dose of 400-keV electrons on the stability of these mixed phases.

Experimental

Hot-pressed ceramic preparations of (Cs,Ba)-hollandite ($Cs_{2.28x}Ba_{1.114(1-x)}Al_{2.29}Ti_{5.71}O_{16}$; $x = 0.20, 0.30$) were prepared by J. Kwiatkowska (*6*) and characterized as hollandite phases by X-ray and neutron powder diffraction and Rietveld refinements (*6*). There was no evidence in these powder data on superstructures due to Cs^{1+}, Ba^{2+}, or vacant-site ordering along the *c*-axis (hollandite tunnel direction) (*6*).

Specimens were examined by HREM at 200 keV in a JEM-200CX, and at 400 keV in a JEM-400EX, at Arizona State University. Polycrystalline ceramic fragments were ground under acetone and dispersed onto holey carbon support films. Thin edges projecting over holes were examined for both [001] and [100] projections. HREM images were monitored continuously using a TV camera viewing a YAG (yttrium–aluminum–garnet) transmission phosphor (supplied by Gatan, CA). Interesting changes under electron irradiation were recorded using a VCR unit. Images were also recorded with Kodak SO-163 film, using 2-sec exposures at 400 keV and electron optical magnifications typically of 600,000×. The current density on the viewing screen, as required for TV recording, was ~50 pA cm^{-2}, equivalent to ca. 10^4 electrons $Å^{-2}$ sec^{-1} at the specimen position.

Results

(*a*) *Electron diffraction patterns.* Both specimens gave identical *c*-axis electron diffraction patterns, as expected for the tetragonal form ($a = 10.04$, $c = 2.95$ Å (*7*)). These patterns showed characteristic, reproducible behavior on examination at both 200 and 400 keV, shown for the 400-keV case in Figs. 1a–c. Thus, after one or two minutes' observation, small square-cross shapes developed at each Bragg spot (Fig. 1b), and these grew in extent following prolonged observation (Fig. 1c). These cross-shaped diffuse streaks are rotated by

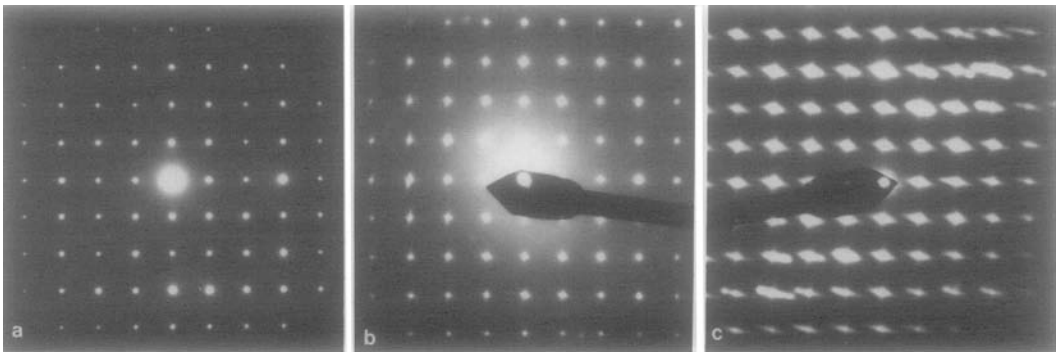

FIG. 1. [001] zone axis electron diffraction patterns of (Cs,Ba)-30% hollandite after observation at 400 keV for (a) 0, (b) 5, and (c) 15 min at an electron dose of ca. 10^4 electrons $Å^{-2}$ sec^{-1}. Note the appearance of faint (b) and then intense (c) streaks through Bragg spots. These are inclined at ca. 10° to [110] and [$1\bar{1}0$] of the originally perfectly sharp pattern (a).

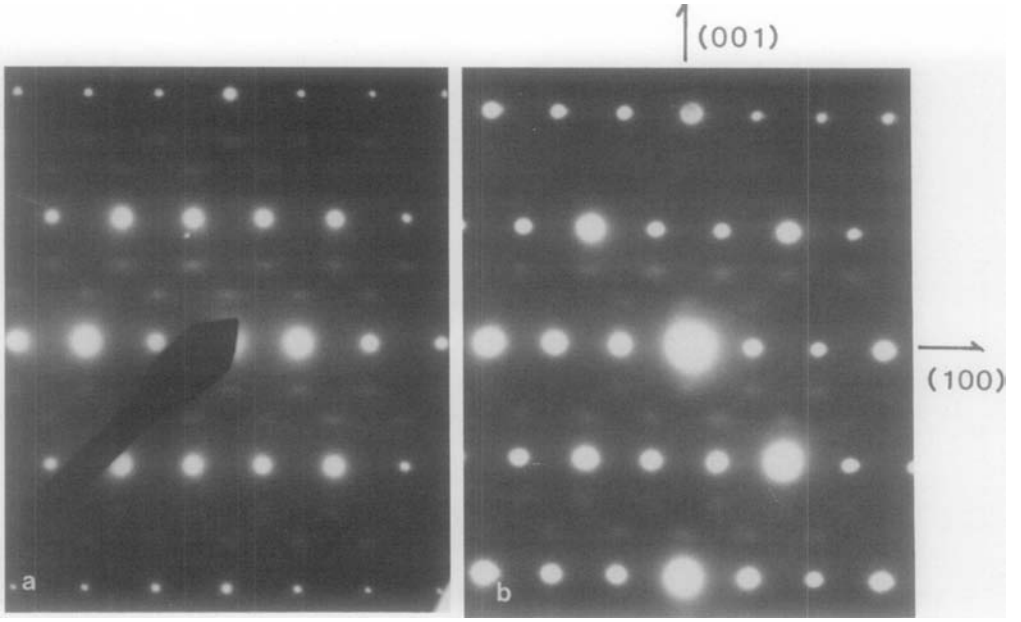

FIG. 2. [010] zone axis electron diffraction patterns for Cs/Ba ratios of 0.30 and 0.20, respectively. Note diffuse incommensurate superlattice scattering with periodicities 2.85× and 2.675× d_{001} in (a) and (b), respectively.

ca. 10° with respect to the ⟨110⟩ axes of the tetragonal cell. The intensity distribution often became quite asymmetrical with one arm of the cross becoming elongated with respect to the other. It is worth noting that similar behavior was reported earlier for ion-thinned specimens of Ba-hollandite (*8, 9*) following prolonged observation of crystal flakes of crushed hollandite (*9*) examined at 200 keV.

[010] axis diffraction patterns for $x = 0.20$ and 0.30 are given in Figs. 2a and b, respectively. This projection, in which the c-axis tunnels lie (exposed) perpendicular to the beam, was not studied in Refs. (*8, 9*). Note the diffuse scattering centered on incommensurate superlattice positions, corresponding to multiplicities of 2.8× and 2.675× d_{001} for $x = 0.30$ and 0.20, respectively. These diffuse scattering distributions are otherwise very similar to each other and to previous observations of pure Ba-hollandites (*7*). The diffuse scattering showed a tendency to spread and diminish in intensity following prolonged (20 min) observation at 400 keV.

(*b*) *HREM observations*. Figure 3a gives a 200-keV image for the [001] projection and $x = 0.30$, recorded before significant beam-induced changes had occurred (cf. the electron diffraction pattern in Fig. 1a). Similar images were obtained for $x = 0.20$. Thus, the image was quite consistent with those expected for tetragonal hollandite-type phases (*10*). Figure 3b gives a 400-keV image for the same projection ([001]) and $x = 0.20$, but recorded for an electron diffraction pattern equivalent to Fig. 1b, when significant beam-induced changes have already occurred. Broad dark fringes appear which crisscross the field of view, and they are inclined at approx. 10° with respect to the basic hollandite ⟨110⟩ directions. Note that in this case the ⟨110⟩ hollandite fringes have so far remained straight and orthogonal. The thin edge of the crystal

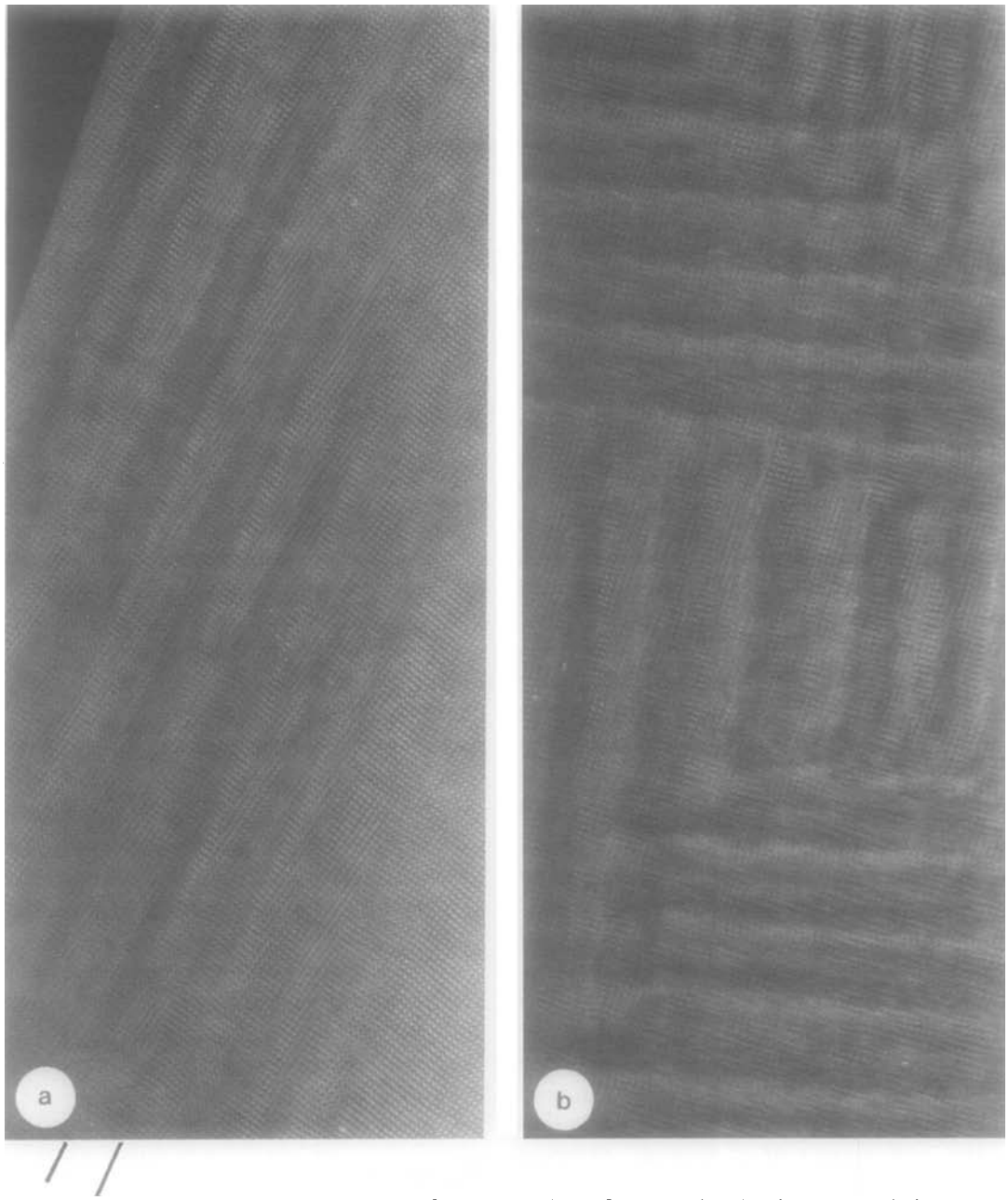

FIG. 3. (a) A 200-keV HREM image for [001] zone axis of (Cs,Ba)-30% hollandite recorded before observable changes occurred due to electron irradiation. (b) A 400-keV HREM image for [001] zone axis of (Cs,Ba)-30% hollandite recorded after slight changes had occurred. Note the entranced structural resolution achieved in (b) compared to (a).

fragment indicates that the structure image condition has been achieved for hollandite, with the larger dark spots in a one-to-one correspondence with the $[MX_6]$ octahedral positions of the transition metal sites, and smaller, less intense, dark spots correspond to the (Cs^{1+},Ba^{2+}) sites within the *c*-axis tunnels of this projection of hollandite (*10*). However, for increasing thickness, there are changes in contrast which are not solely due to thickness variations: squarish shapes appear (approx. 50 × 50 Å^2 in area) which show sharp changes in symmetry and details of the image, and these represent the first visible beam-induced changes in structure. Note that there are significant advantages in using an accelerating voltage of 400 keV, as far as the image quality and interpretability are concerned (cf. Figs. 3a and b). Thus, the structure image condition is more readily achieved and apparent at 400 keV.

[001] images from the same area of a crystal were recorded at 400 keV after different periods of observation. Thus, unidirectional (50 Å) broad fringes appeared after ca. 5 min (Fig. 4a) whereas a two-dimensional superstructure (50 × 50 Å^2) appeared after ca. 15 min (Fig. 4b). Figures 5a, b, and c show high-resolution image detail for specimens examined for ca. 5, 15, and 30 min, respectively (beam current ~50 pA cm^{-2} on the viewing screen at 400 keV). Note the thin edges in Fig. 5a. Observation along the ⟨110⟩ directions shows that the structure is no longer tetragonal and the interaxial angle [110]–[1$\bar{1}$0] has changed from 90 to 100° or from 90 to 80°, giving rise to the appearance of a multiply twinned texture. In thicker regions, the broad band contrast appears, but the complexity of the lattice images is no longer directly interpretable (cf. Figs. 4a and b). Further irradiation (Fig. 5b) results in the appearance of a disordered surface layer with effects varying from lowering of symmetry, in the lattice image, to the appearance of apparently amorphous regions at the thinnest edges. After 30 min (Fig. 5c), the amorphous edge is more extensive. Small patches of fringes occur, having spacings and orientations different from those present originally. There is also evidence for loss of material (sputtering) in the form of whiter (thinner) patches.

A 400-keV image for the [010] projection, characteristic of the as-prepared material, is shown in Fig. 6a. Note the appearance of contrast fluctuations, small whiter and darker spots superimposed upon the average lattice image, dotted apparently randomly, throughout the image. Sighting at a glancing angle along the direction arrowed shows weak darker fringes (average spacing ≈15–20 Å) which waver across the specimen, with ill-defined orientation and spacing. These correlate with the brighter and darker spots referred to above, indicating that there is actually considerable short-range correlation in their distribution. Further [010] HREM images recorded after observation at 400 keV for ca. 5, 15, and 30 min respectively are shown in Figs. 6b–d. Continued degradation (or glassification) of the hollandite structure is again apparent, with initial changes of symmetry and loss of tunnel image detail, development of patches of fringes having different spacings and orientations, and, finally, continued growth of noncrystalline surface layers.

It is noteworthy that the electron-beam-induced changes are not only visible more readily at 400 than at 200 keV but appear at a significantly greater rate.

Discussion

(*a*) (*Cs,Ba*) *distribution*. The incommensurate superlattice structures of Ba-hollandite have been discussed in detail elsewhere (*7*). The periodicities shown by the diffuse superstructures in Figs. 2a and b were 2.67× and 2.875× d_{001} for $x = 0.20$ and 0.30, respectively. A recent paper (*11*)

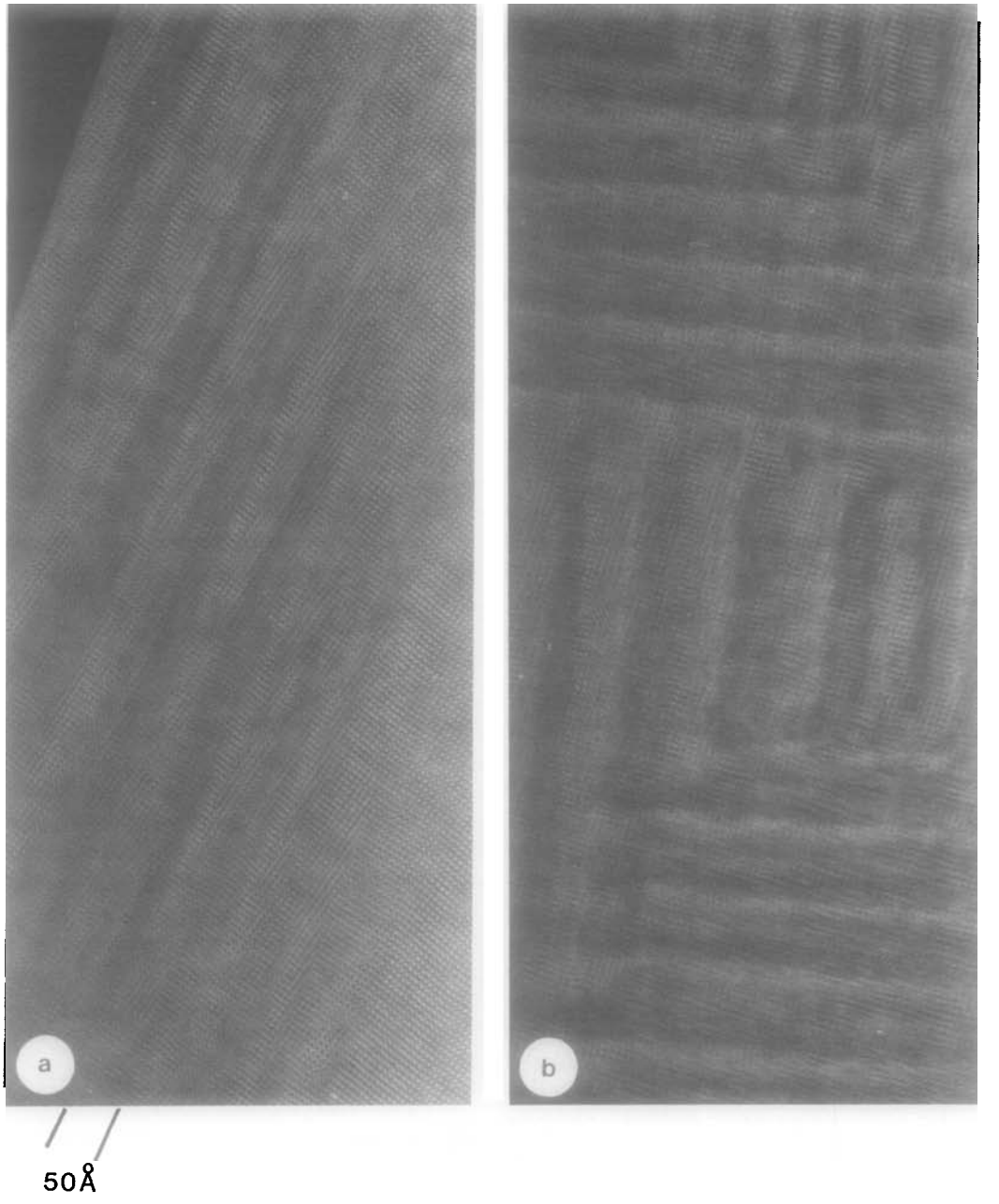

FIG. 4. (a) One-dimensional and (b) two-dimensional textures appearing in (Cs,Ba)-20% hollandite after examination at 400 keV for 5 and 15 min, respectively. Broad diffuse changes in the background occur with periodicities of 50, within which states or blocks of contrast develop having distinct changes in symmetry and fine detail compared with the original unirradiated specimens (cf. Fig. 3).

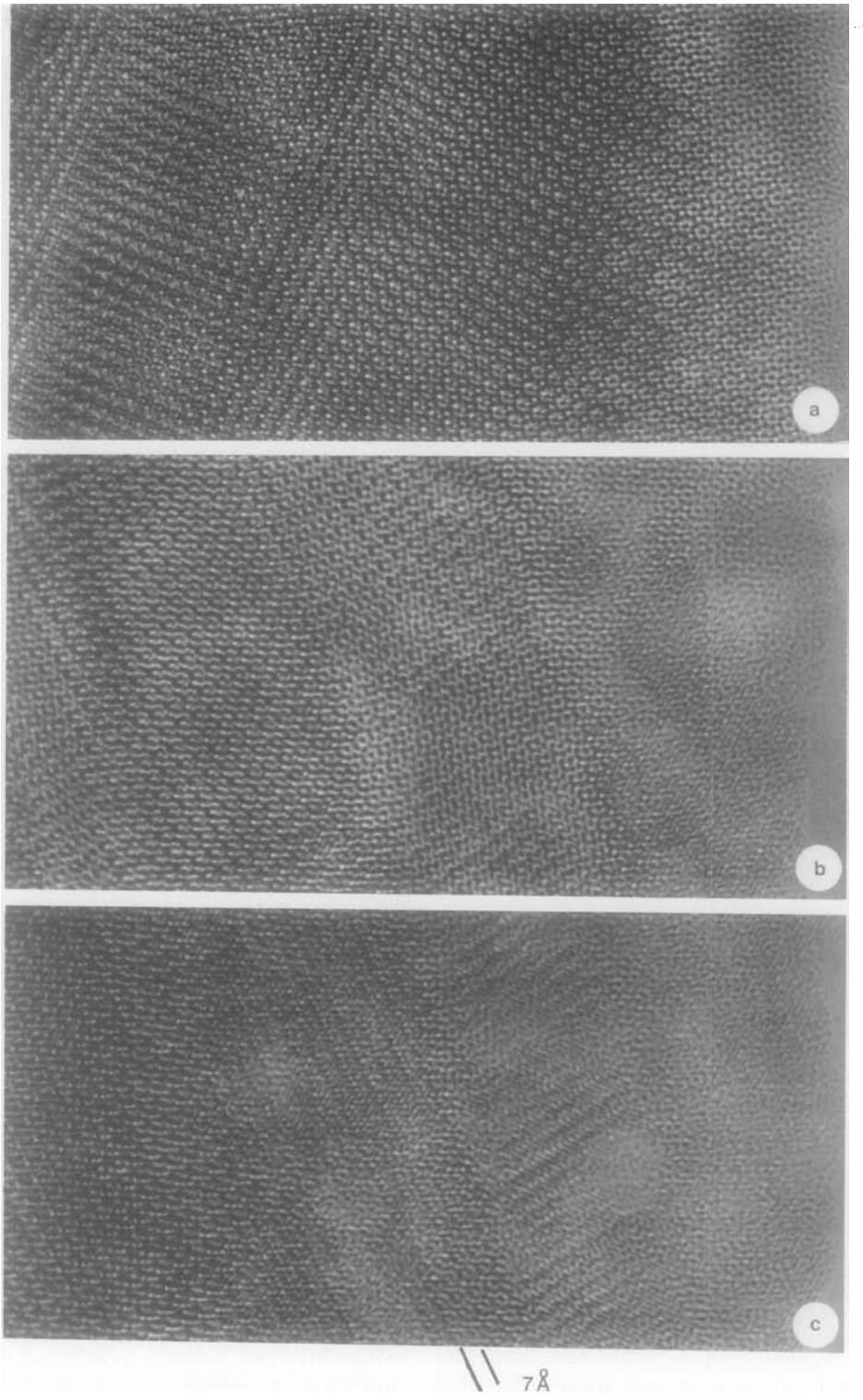

FIG. 5. [001] zone axis images of (Cs,Ba)-20% hollandite after examination times of (a) 5, (b) 15, and (c) 30 min. Note degradation of edge regions, with first changes in symmetry and loss of tunnel image in (a) and (b), followed by apparent amorphization in (b) and (c).

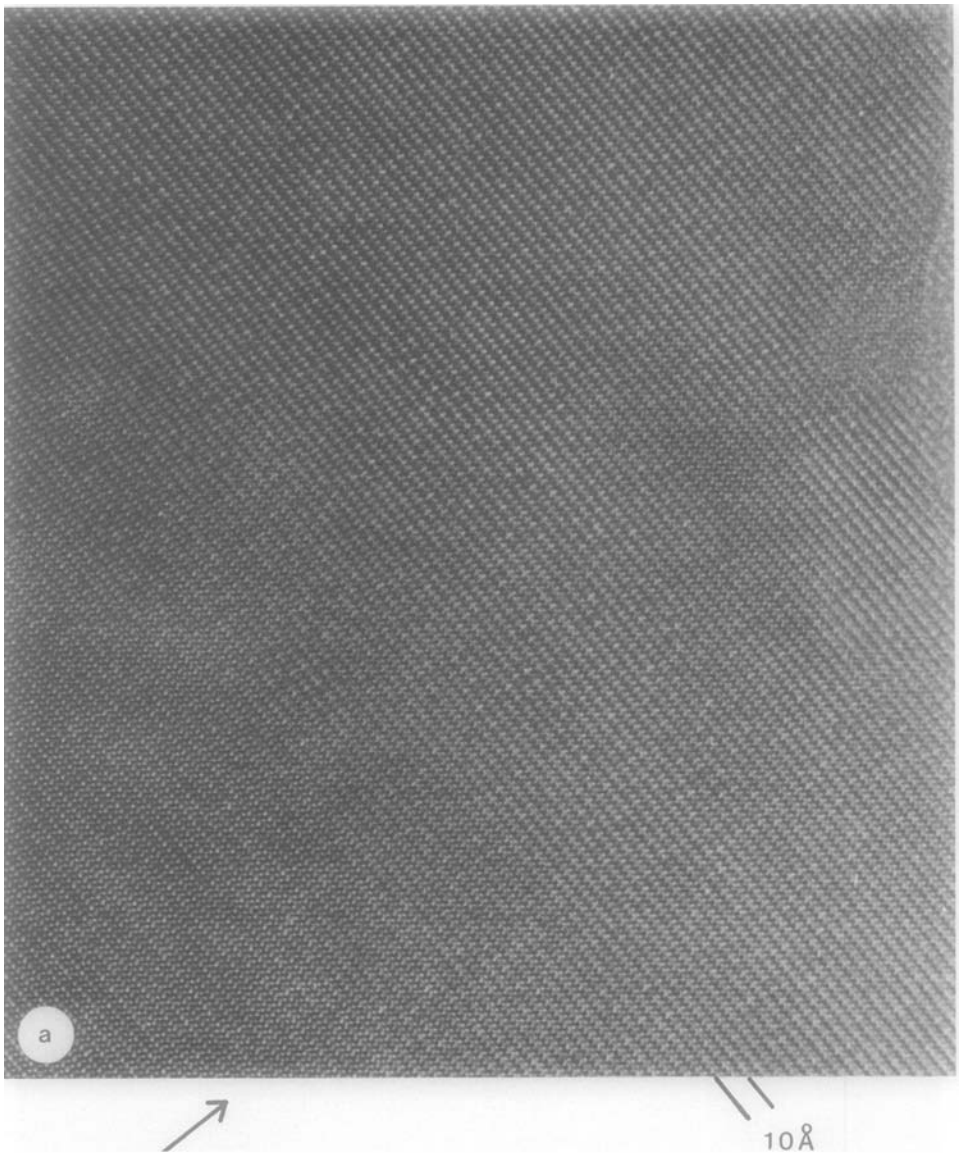

FIG. 6. (a) HREM image of (Cs,Ba)-20% hollandite for [010] projection recorded before significant beam-induced changes occurred. Note quasi-regular distribution of white and dark variations of spot intensity along the c-axis tunnels. The presence of significant short-range-order correlations may be seen most readily by sighting along the direction of the arrow. (b), (c), and (d) show degradation of the structure following electron beam irradiation for 5, 15, and 30 min, respectively. Note appearance of different crystalline structure images near the thin edges after 5 and 15 min (b and c) and finally apparent amorphization of the surface layers after 15 and 30 min (c and d).

gives evidence of x-values less than the nominal values expected from solid-state synthesis. A $3\times$ d_{001} superstructure corresponds to two-thirds occupancy of the hollandite-type tunnels, yielding a stoichiometry of $A_{1.67}M_8O_{16}$ (*7*), whereas the as-prepared stoichiometries used in the present study were nominally $A_{1.482}M_8O_{16}$ (x =

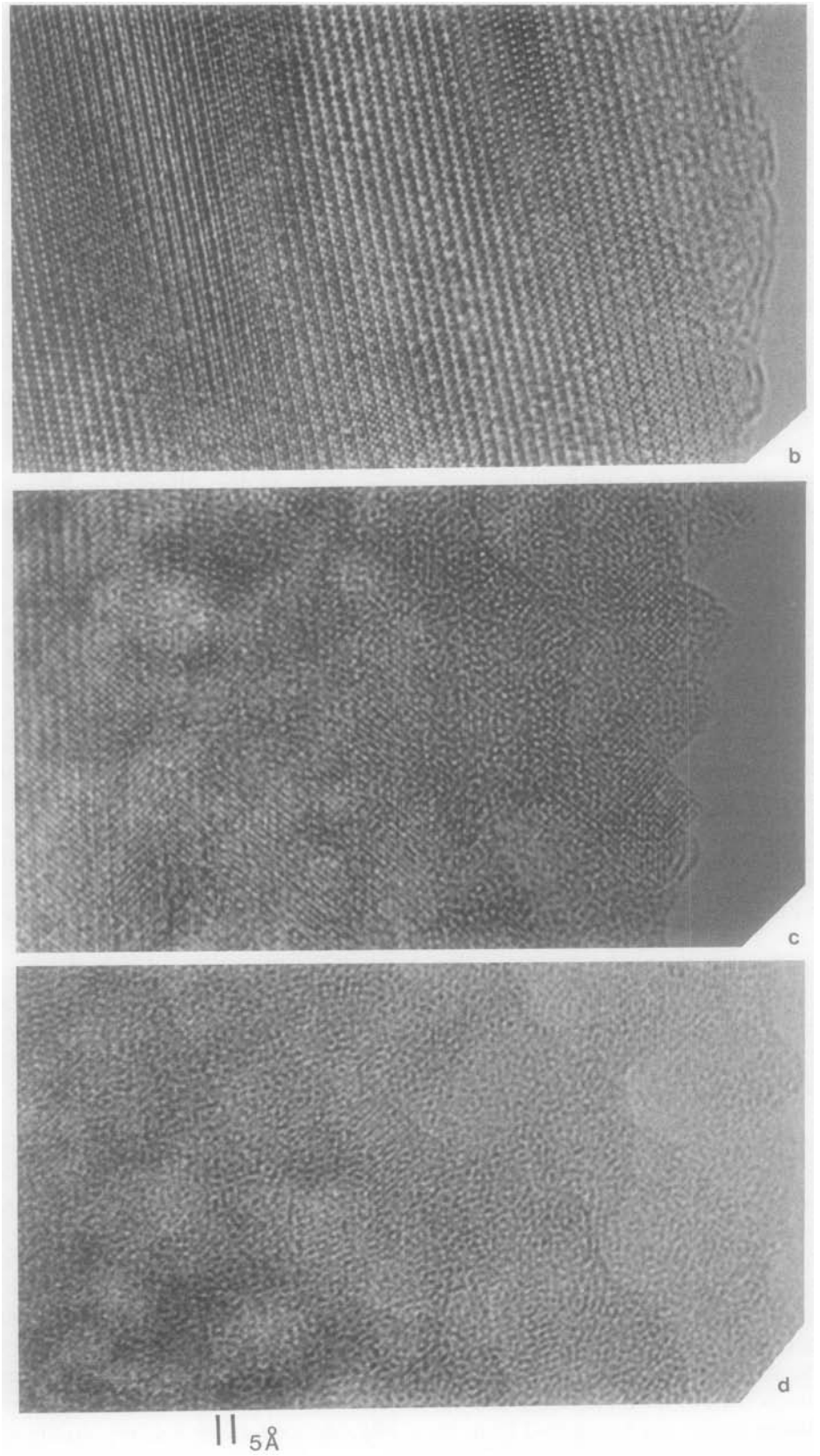

FIG. 6—*Continued.*

0.30) and $A_{1.368}M_8O_{16}$ ($x = 0.20$). In each case, vacant tunnel sites occur relative to the ideal $3\times$ d_{001} superstructure. Thus, the longer incommensurate periodicity $2.8\times$ for $x = 0.30$, relative to 2.67 for $x = 0.20$, simply corresponds to the larger mean separation of vacancies expected for $x = 0.30$ compared with $x = 0.20$. The black and white fluctations observed across the HREM images of both $x = 0.20$ and 0.30 preparations (cf. Fig. 6a) presumably represent fluctuations in vacancy concentrations rather than indicating the distribution of Cs and Ba ions, since it is unlikely that Cs^{1+} and Ba^{2+} could be distinguished in HREM images. There is no evidence for other than a classical solid solution distribution for the mixed (Cs,Ba) site occupancies in our preparations, at least before they are subjected to significant electron irradiation.

(*b*) *Electron irradiation.* Degradation of the (Cs,Ba)-hollandite structure under electron irradiation is clearly demonstrated in Figs. 5 and 6, although details of the structural changes are complex and not readily interpreted. Even the chemical nature of the surface layers remains unknown at present, since preferential volatilization of Cs^{1+} with respect to Ba^{2+} and/or preferential loss of oxygen (O_2) with respect to (Ti,Al) may be involved.

The 0.518- and 1.218-MeV β^--particles emitted by radioactive decay of $^{137}Cs^{1+} \rightarrow {}^{137}Ba^{2+} + \beta^-$ both have energies higher than the 400-keV electrons used in the present study. All three energies are above threshold energies for direct displacement of cations and oxygen anions in many crystalline phases (*12*). However, several electron-beam-induced (ebd) decomposition mechanisms have threshold energies $\leq$30 eV, corresponding to electronic excitations in and about the band gap (*12*). Such ebd mechanisms are especially effective close to the surfaces of solids, since an anion (or a cation) may acquire extraordinary charge states and be ejected from the surface due to the consequent electrostatic instability of its interatomic bonds with neighboring ions. These electronic-induced decompositions remain controversial and incompletely understood (*12*).

The microtwinning observed in surface layers of (Cs,Ba)-hollandites (see Figs. 3 and 6) suggests that an initial effect of electron irradiation is the displacement of Cs ions from the square tunnels present in tetragonal hollandites, leaving the tunnels susceptible to a shear deformation. Such deformations occurred in the phase $Ba_2Ti_9O_{20}$ (*13*). In fact, $Ba_2Ti_9O_{20}$ has approximately a close-packed arrangement of (Ba^{2+},O^{2-}) ions, including mixed (Ba^{2+},O^{2-}) ion occupancies in the sheared-tunnel part of this hollandite-related phase. The observed shear angle ($\sim$10°) and the image contrast for both [001] and [010] projections after 5- to 15-nm irradiation (Figs. 5 and 6) are strongly suggestive of a structurally similar beam-induced transformation. Thermal decomposition (or unmixing) of the (Cs,Ba)-hollandite into $Ba_2Ti_9O_{20}$ + $Cs_2Ti_5O_{11}$ phases has been reported earlier (*14*). The characteristic lath-like or fibrous texture adopted by $Cs_2Ti_5O_{11}$ has been described recently (*15*), but no direct evidence for its presence was found in the present study.

For pure ^{137}Cs, there is a concentration of 2×10^{-3} $^{137}Cs^{1+}$ ions per cubic angstrom, since each $10 \times 10 \times 3$-Å^3 unit cell contains two (Cs,Ba) sites. Assuming that each $^{137}Cs^{1+}$ ion decays after a period of 10 half-lives (i.e., 300 years) gives a net dose of 4×10^{-3} electrons Å^{-3} or 4.16×10^{-7} electrons Å^{-3} sec^{-1}. The range of 0.5- to 1.2-MeV electrons may be $\sim$10 μm so that virtually all the β-particles will remain inside a bulk ceramic preparation. The equivalent dose of electrons incident on a 1-m-thick transmission electron microscope specimen would, therefore, be ca. 40 electrons Å^{-2} at the entrance surface. Actually, the two cases are not strictly compa-

rable, since the incident beam divergence is only 0.5 mrad for typical HREM illumination conditions, whereas the above figure of 4×10^{-7} electrons $Å^{-3}$ sec^{-1} for β-decay is integrated over all directions of incidence. *In situ* HREM observations may, therefore, overemphasize directional effects and it is not meaningful to try to define the equivalent doses for the self-irradiation by β-decay of bulk hollandites compared with electron-beam irradiation of thin foils (1000 Å thick) of hollandite in HREM. The power density for the latter is certainly extremely high, having been likened to that existing inside a thermonuclear explosion (*16*). Thus, electron current densities at the sample of $j_p \approx 10^2$–10^7 A m^{-2} are typical so that the energy *deposited* by *inelastic* scattering may be typically 1 kW–1 MW mm^{-3} (*12*). This converts to between 10 and 10^6 electrons $Å^{-2}$ sec^{-1} for a 1000-Å foil. These (very rough) figures suggest that hollandite irradiated at 400 kV for ≈1 min experiences a dose of high-energy electrons far in excess of that received by a typical SYNROC hollandite in 300 years. Clearly, the changes observed above may well be compounded by rate-dependent effects, compared with self-irradiation processes at a much lower dose rate.

Conclusion

In view of the above observed sensitivity of (Cs,Ba)-hollandite preparations to electron beam irradiation at 400 kV, with a loss of crystallinity at least in the surface layers and possible chemical and mechanical instabilities consequent to this, it seems desirable to undertake further research on the stability of SYNROC preparations under irradiation.

Short of examining "hot" hollandite preparations at intervals of the order of one half-life (30 years) it would seem desirable, nevertheless, to simulate the possible self-irradiation effects of β-decay using high-energy electrons in the laboratory. This occurred more or less fortuitously in the present study due to the recent availability of a high-resolution 400-kV instrument.

There is a need for a comprehensive study, perhaps using a dedicated variable-energy instrument having higher energies (0.518 and 1.218 MeV) and using special facilities to enable long-term irradiation at a lower rate. The detailed nature and origin of the observed degradation of hollandite, for both electron and ion irradiation, need further investigation.

If the present experimental observations do nothing else, they serve to emphasize how little is known about the underlying radiation physics and chemistry of SYNROC and similar radwaste proposals.

Acknowledgments

The work was supported by the Australian Research Grants Committee, the University of Melbourne, and the NSF under Grant DMR-8306501 to the Facility for High-Resolution Electron Microscopy in the Center for Solid State Science, Arizona State University. We are grateful to Dr. Ed Muirhead (Melbourne) and Professor J. M. Cowley (ASU) for support of visits to ASU (by L.A.B.) and to Melbourne (by D.J.S.).

References

1. A. E. Ringwood, S. E. Kesson, N. G. Ware, W. O. Hibberson, and A. Major, *Geochem. J.* **13,** 141 (1979).
2. Y. Fujibi, Yū Komatsu, T. Sasaki, and N. Ohta, *J. Chem. Soc. Japan* **10,** 1656 (1981) [in Japanese]; see also *Chem Lett.* (1980), 0.1023–26.
3. L. A. Bursill, *J. Solid State Chem.*, in press.
4. G. Bayer and W. Hoffman, *Amer. Mineral.* **51,** 511 (1966).
5. R. Roth, *in* Annual Report, NBS1R-81-2241, p. 42, National Measurement Laboratory Office of Measurements for Nuclear Technology (1981).
6. J. Kwiatkowska, Ph.D thesis, University of Melbourne (1985); see also R. W. Cheary, J. V. Hunt, and P. Calaizis, *J. Austral. Ceram. Soc.* **17,** 11–12 (1981), and R. W. Cheary and J. Kwiatkowska, *Nucl. Mater.* **125,** 236–243 (1984).

7. L. A. BURSILL AND G. GRZINIC, *Acta Crystallogr., Sect. B* **36,** 2902 (1980).
8. T. J. HEADLEY, *in* "39th Annual Proceedings, Electron Microscope Society of America, Atlanta, Georgia, 1981" (G. W. Bailey, Ed.), p. 114, Claitor's, Baton Rouge, LA (1981).
9. J. C. BARRY, J. L. HUTCHINSON, AND R. L. SEGALL, *J. Mater. Sci.* **18,** 1421 (1983).
10. L. A. BURSILL AND A. R. WILSON, *Acta Crystallogr., Sect. A* **33,** 672 (1977).
11. R. W. CHEARY, *Acta Crystallogr., Sect. B* **42,** 229–236 (1986).
12. L. W. HOBBS, *in* "Introduction to Analytical Electron Microscopy" (J. J. Hren, J. C. Goldstein, and D. C. Joy, Eds.), Chap. 17, Plenum, New York (1979).
13. G. GRZINIC, L. A. BURSILL, AND D. J. SMITH, *J. Solid State Chem.* **47,** 151 (1983).
14. L. A. BURSILL AND J. KWIATKOWSKA, *J. Solid State Chem.* **52,** 45 (1984).
15. L. A. BURSILL, J. KWIATKOWSKA, AND D. J. SMITH, *J. Solid State Chem.* **69,** 360 (1987).
16. Attributed to Professor Sir Charles Frank, FRS.